evidence that these sites are initially open and accessible, but that compaction of the complex occurs upon binding of ribosomal proteins.

It is not clear why Stuhrmann plots for non–salt-washed subunits have such a large slope and a consequently large value of the protein R_g while subunits salt-washed to remove protein S1 do not. It is unlikely that the S1-depleted and reconstituted species studied here have suffered a partial loss of ribosomal proteins, because both of these species are fully active and have measured contrast match-points that are identical within error to calculated values. S1 has been located close to the protein center of mass (*16*) and therefore should not make a large difference to the protein R_g. Sodium dodecyl sulfate gels (Fig. 1b) on the subunits with S1 show the presence of several bands corresponding to nonribosomal proteins that are not present in the salt-washed or reconstituted subunits. The match-point for the subunits with S1 is also slightly lower than calculated; this leads to an estimate of about 11 percent more protein than would be expected from a unit stoichiometry of the 21 ribosomal proteins. Thus it is likely that nonribosomal proteins are bound to the region of RNA that is farthest from the protein center of mass, giving rise to a spuriously large R_g for the protein component. On the other hand, in at least one previous report (*6*), the subunits studied were washed in 0.5*M* NH_4Cl. The possibility remains, therefore, that the location of S1, which was determined by measuring the distance of cross-linked S1 to other ribosomal proteins, is erroneous.

In any case, with the possible exception of protein S1, the proteins and RNA of the 30*S* ribosomal subunit are intermingled, but are asymmetric in their spatial distribution, with a center of mass separation of 25 Å. These findings offer direct and independent evidence that the picture of the small subunit that is emerging from efforts to locate individual ribosomal proteins is correct with respect to the overall distribution of protein and RNA.

REFERENCES AND NOTES

1. K. Ibel and H. B. Stuhrmann, *J. Mol. Biol.* **93**, 255 (1975).
2. M. H. J. Koch and H. B. Stuhrmann, *Methods Enzymol.* **59**, 670 (1979).
3. P. B. Moore, D. M. Engelman, B. P. Schoenborn, *J. Mol. Biol.* **91**, 101 (1975).
4. P. Beaudry, H. U. Petersen, M. Grunberg-Manago, B. Jacrot, *Biochem. Biophys. Res. Commun.* **72**, 391 (1976).
5. H. B. Stuhrmann *et al.*, *J. Mol. Biol.* **119**, 203 (1978).
6. I. N. Serdyuk, A. K. Grenader, G. Zaccai, *ibid.* **135**, 691 (1979).
7. P. B. Moore *et al.*, in *Structure, Function and Genetics of Ribosomes*, B. Hardesty, Ed. (Springer, New York, in press).
8. L. Kahan, D. A. Winkelmann, J. A. Lake, *J. Mol. Biol.* **145**, 193 (1981).
9. B. Kastner, M. Noah, M. Stoffler-Meilicke, G. Stoffler, *Proc. 10th Int. Congr. Electron. Microsc.* **93**, 99 (1983).
10. P. B. Moore, *Methods Enzymol.* **59**, 639 (1979).
11. J. A. Steitz, A. J. Wahba, M. Laughrea, P. B. Moore, *Nucleic Acids Res.* **4**, 1 (1977).
12. R. F. Gesteland, *J. Mol. Biol.* **18**, 356 (1966).
13. D. Schneider and B. P. Schoenborn, in *Neutrons in Biology*, B. P. Schoenborn, Ed. (Plenum, New York, 1984), pp. 119–142.
14. S. I. Edelstein and H. K. Schachman, *Methods Enzymol.* **27**, 82 (1973).
15. I. Serdyuk *et al.*, *J. Mol. Biol.* **169**, 409 (1983).
16. I. Y. Sillers and P. B. Moore, *ibid.* **153**, 761 (1981).

17. Research was carried out under the auspices of the U.S. Department of Energy. I thank D. Schneider for his help with these experiments, P. B. Moore for a gift of deuterated RNA, and B. P. Schoenborn for his encouragement. I thank R. M. Sweet for a critical reading of this manuscript.

12 August 1985; accepted 16 December 1985

Calcium Channels in Planar Lipid Bilayers: Insights into Mechanisms of Ion Permeation and Gating

ROBERT L. ROSENBERG, PETER HESS, JOHN P. REEVES, HENRY SMILOWITZ, RICHARD W. TSIEN

Electrophysiological recordings were used to analyze single calcium channels in planar lipid bilayers after membranes from bovine cardiac sarcolemmal vesicles had been incorporated into the bilayer. In these cell-free conditions, channels in the bilayer showed unitary barium or calcium conductances, gating kinetics, and pharmacological responses that were similar to dihydropyridine-sensitive calcium channels in intact cells. The open channel current varied in a nonlinear manner with voltage under asymmetric (that is, physiological) ionic conditions. However, with identical solutions on both sides of the bilayer, the current-voltage relation was linear. In matched experiments, calcium channels from skeletal muscle T-tubules differed significantly from cardiac calcium channels in their conductance properties and gating kinetics.

CALCIUM CHANNELS ARE VITAL TO neurotransmission, secretion, and muscle contraction and are important targets of neurochemical modulators (*1*). The molecular properties of Ca^{2+} channels have been studied with single-channel recordings in intact cells (*2–6*) and with biochemical investigations of putative Ca^{2+} channel proteins (*7*). These different approaches to channel function and structure can be combined by studying Ca^{2+} channels under cell-free conditions where the lipid and ionic environment can be controlled. This can be done by recording the activity of Ca^{2+} channels incorporated into planar bilayers (*8–10*). However, there has been no direct comparison of single-channel properties in planar bilayers and in intact cells under matched experimental conditions. Here we report that cardiac Ca^{2+} channels reconstituted in artificial membranes and Ca^{2+} channels in intact heart cells have similar properties of ion permeation and gating. We have also been able to gain new information about the mechanism of ion permeation by using this technique to study calcium channels under experimental conditions unattainable in intact cells. Furthermore, we find that Ca^{2+} channels from skeletal muscle T tubules and cardiac sarcolemma differ significantly in single-channel conductance and gating despite their common sensitivity to dihydropyridines.

Unitary Ca^{2+} channel activity was observed after incorporation of cardiac sarcolemmal vesicles into a lipid bilayer (Fig. 1A) (*11*). The external side to the channel was exposed to 100 m*M* Ba^{2+} and 50 m*M* Na^+ and the internal side to 50 m*M* Na^+ and no Ba^{2+}. In these studies, channel sidedness is defined such that positive internal potentials promote channel openings (*12*). The dihydropyridine (DHP) Ca^{2+} agonist Bay K 8644 (*13*) was included in all experiments to promote long openings of L-type Ca^{2+} channels (*6, 14, 15*). Membrane depolarizations to +10 mV evoked channel activity (Fig. 1A) that was seen as inward current pulses of ~1.2 pA. This current must have been carried by Ba^{2+} ions because Ba^{2+} was the only ion present that had an inwardly directed driving force at +10 mV. The slope conductance at 0 mV was 23 picosiemens (pS). In experiments with 100 m*M* external Ca^{2+}, unitary current events at +10 mV were only ~0.4 pA, and the slope conductance was ~7 pS. These amplitudes of elementary currents are typical for cardiac L-type Ca^{2+} channels in cell-attached patches (*3, 5, 15*).

R. L. Rosenberg, P. Hess, R. W. Tsien, Department of Physiology, Yale University School of Medicine, New Haven, CT 06510.
J. P. Reeves, Roche Institute of Molecular Biology, Nutley, NJ 07110.
H. Smilowitz, Department of Biochemistry, University of Connecticut, Farmington, CT 06032.

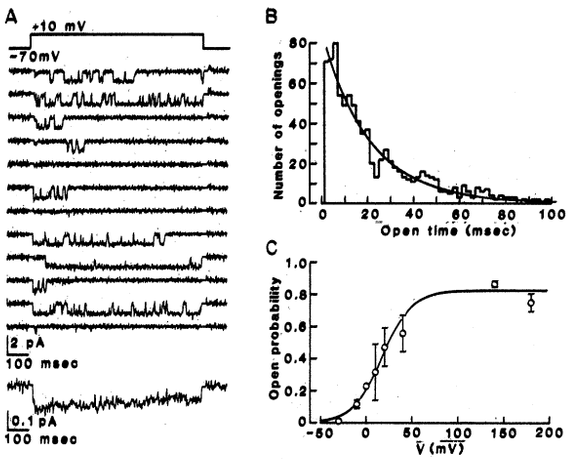

Fig. 1. Cardiac Ca^{2+} channels in planar bilayers. Extracellular solution contained 50 m*M* NaCl, 100 m*M* $BaCl_2$, 1 m*M* EDTA, 10 m*M* 4-(2-hydroxyethyl)-1-piperazineethane sulfonic acid (Hepes)–NaOH, *p*H 7.4; intracellular solution contained 50 m*M* NaCl, 1 m*M* EDTA, 10 m*M* Hepes-NaOH, *p*H 7.4 (*12*). Bay K 8644 (1 μ*M*) was present on both sides. (A) Current records from a bilayer containing a single Ca^{2+} channel (*11*). Voltage-clamp depolarizations from −70 mV to +10 mV were applied every 2 seconds. Channel openings are shown as a downward transition. Linear leakage and capacity currents have been subtracted. The average of 120 records is shown below the individual current traces. Data are from bilayer J5D1. (B) Channel open time distribution at 0 mV. Opening and closing events were detected by setting a discriminator at 50 percent of the single-channel current. The smooth curve is the least-squares fit of the data with a single exponential (time constant, 20 msec) (*18*). Bilayer J5P3. (C) Open probability as a function of test potential. Open probability was determined for each sweep containing channel activity; null sweeps were excluded. The average probability and standard errors at each potential were plotted. Holding potential was −80 mV. The smooth curve was drawn according to the equation $P_{open} = 0.825/\{1 + \exp[(18\ mV - V)/16\ mV]\}$. Bilayer J4Y5.

Individual current traces were averaged to give a mean current record (Fig. 1A, bottom) that activated rapidly following depolarization, inactivated slowly during a maintained depolarization, and deactivated very rapidly following repolarization. The kinetics of channel gating were typical for Ba^{2+} currents through cardiac L-type Ca^{2+} channels in the presence of Bay K 8644 (*6, 14*). In experiments where Ca^{2+} carried the inward current, inactivation was significantly faster, in agreement with results from intact cells (*16*). The mean open time with Ba^{2+} was ~20 msec (Fig. 1B), as expected for long-lasting channel openings promoted by Bay K 8644 (*6, 14, 17*). Brief openings, which dominate L-type channel gating in the absence of DHP Ca^{2+} agonists (*3, 5, 6*), were largely filtered out by the bandwidth limitations of the bilayer recordings (*18*). The voltage-dependence of channel activation is shown in Fig. 1C. The steepness and the voltage range of activation were characteristic of cardiac L-type channels in intact cells (*3, 5*).

Calcium channels in planar bilayers responded to pharmacological agents known to inhibit L-type Ca^{2+} channels in intact cells. Addition of the DHP Ca^{2+} antagonist nimodipine (6 μ*M*) to both sides of the planar bilayer completely abolished Ca^{2+} channel activity despite the presence of Bay K 8644 (1 μ*M*). External cadmium ions reduced the apparent unitary current amplitude (*19*) and increased the open-channel noise, as expected for fast "flickery" block (*20*). In the presence of 100 m*M* Ba^{2+}, the unitary currents were reduced to 50 percent of control at ~30 μ*M* Cd^{2+}, in excellent agreement with results in cell-attached patches (*20*).

In perhaps the most stringent test, we compared directly the voltage-dependence of the open channel current of Ca^{2+} channels in planar bilayers and intact cells under closely matched ionic conditions (Fig. 2A). The current-voltage (I-V) relations could almost be superimposed in the intermediate voltage range where currents could be measured with both experimental designs (23 pS at 0 mV). In bilayers as well as cell-attached patches, the reversal potential was close to +100 mV, corresponding to a Fatt-Ginsborg permeability ratio of $P_{Ba^{2+}}/P_{K^+} = 2800$ (*21*).

Because the artificial membranes were more stable at very strong depolarizations than were cell-attached patches, we were able to record unitary outward currents carried by internal K^+ (Fig. 2A) or internal Na^+ (Fig. 2B, closed circles). In both cases, the slope conductance for the outward currents increased steeply with voltage, producing an asymmetric, strongly inflected I-V relation. To determine whether this nonlinearity was a consequence of the asymmetric distribution of ions or whether the channel itself was functionally asymmetric, we measured the open channel I-V relationship with symmetric ionic conditions (Fig. 2B, open circles). As expected, the reversal potential was 0 mV. On either side of the reversal potential, inward and outward currents were equal and opposite. Thus, the open channel behaves like a functionally symmetric pore under these symmetric ionic conditions. The linearity of the I-V relation with symmetric Ba^{2+} is in sharp contrast to the nonlinearity seen with external Ba^{2+} and internal monovalent ions (Fig. 2, A and B, closed circles). The steeply increasing conductance for outward monovalent current likely reflects a voltage-dependent decrease of channel occupancy by Ba^{2+} (*22*). Interestingly, the unitary outward currents carried by Na^+ are significantly larger than those carried by K^+, despite the higher internal K^+ concentration (compare Fig. 2, A and B). These results provide support for the idea that these Ca^{2+} channels select among monovalent ions, as well as among divalent ions (*22*).

Although cardiac L-type Ca^{2+} channels have been extensively studied at the single-channel level, they have not yet been purified. Efforts at purification have focused mainly on Ca^{2+} channels from skeletal muscle T-tubules (*7*) which are not accessible to patch clamp recordings. Since single-channel recordings can be made from skeletal muscle Ca^{2+} channels incorporated into lipid bilayers (*9*), a direct comparison between the two types of channels can now be made.

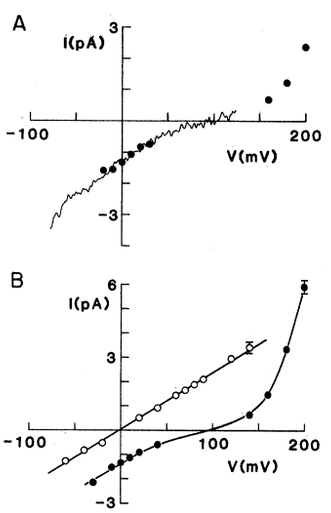

Fig. 2. Cardiac Ca^{2+} channel current-voltage relations. (A) Current-voltage relations for a cell-attached patch (line) and a planar bilayer (points). The cell-attached patch I-V relation was obtained with a voltage ramp command as described in (*20*). Pipette solution contained 110 m*M* $BaCl_2$, 10 m*M* Hepes–tetraethyl ammonium hydroxide (TEAOH), *p*H 7.4. The cell membrane potential outside the patch was zeroed by an external solution containing 140 m*M* potassium aspartate, 10 m*M* EGTA, 1 m*M* $MgCl_2$, and 10 m*M* Hepes-TEAOH plus 1 μ*M* Bay K 8644. In the planar bilayer experiments, the extracellular solution contained 110 m*M* $BaCl_2$, 10 m*M* Hepes-NaOH, *p*H 7.4, and the intracellular solution contained 150 m*M* KCl, 1 m*M* EDTA, 10 m*M* Hepes-NaOH, *p*H 7.4. Holding potential was −80 mV. Data are from bilayers J5F1, J5G1, and J5N1. Standard errors are shown when they were larger than the symbols. (B) Current-voltage curves for reconstituted Ca^{2+} channels exposed to symmetric solutions of 100 m*M* $BaCl_2$, 50 m*M* NaCl, 1 m*M* EDTA, 10 m*M* Hepes-NaOH, *p*H 7.4 (○), or asymmetric solutions containing 100 m*M* $BaCl_2$, 50 m*M* NaCl outside, and 50 m*M* NaCl inside (Fig. 1) (●). Curve was drawn by eye; straight line is the least-squares fit of the data. Bilayers J4Y5 and J5H1.

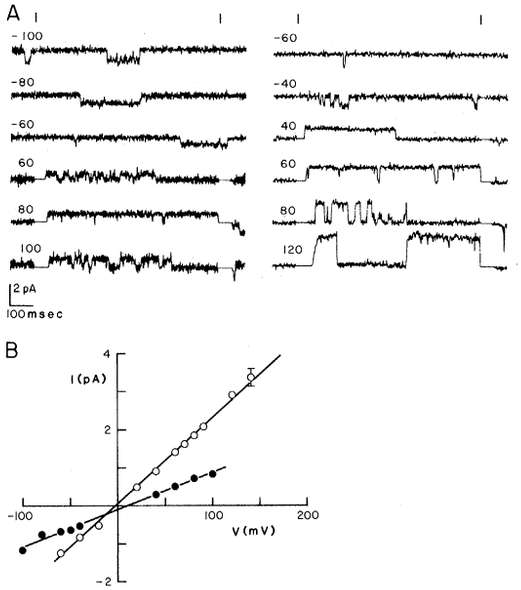

Fig. 3. Comparison of cardiac and skeletal muscle Ca^{2+} channels with symmetric solutions of 100 m*M* $BaCl_2$, 50 m*M* NaCl, 10 m*M* Hepes-NaOH, *p*H 7.4. (A) (Left) Skeletal muscle T-tubule Ca^{2+} channel records (*11*). Holding potential was −100 mV; the vertical marks indicate the start and termination of depolarizations to the test potentials shown. Data are from bilayer R3A1. (Right) Cardiac Ca^{2+} channel records. Holding potential was −80 mV. Bilayer J5H1. (B) Current-voltage curves of cardiac (○) and skeletal (●) Ca^{2+} channels. Lines are the least-squares fits of the data points.

Figure 3 compares individual current traces and open channel I-V relations under identical ionic conditions. With 100 m*M* Ba^{2+} plus 50 m*M* Na^+ on both sides of the bilayer, the skeletal muscle Ca^{2+} channel has a conductance (10.6 ± 0.8 pS, mean ± SEM, $n = 3$) that is significantly smaller than that of the cardiac L-type Ca^{2+} channel (22.7 ± 1.1 pS, $n = 4$). In addition to this difference in ion conductance, we find major differences in the gating behavior of channels from skeletal and cardiac muscle (Fig. 3). Under the ionic conditions of the bilayer experiments, activity of the skeletal muscle Ca^{2+} channel can be seen at −100 mV (Fig. 3) where there is essentially no activity of the cardiac channel. The skeletal channels activate more slowly and have a longer mean open time. These differences in single-channel properties suggest structural diversity even among Ca^{2+} channels that share sensitivity to dihydropyridines.

In summary, cardiac Ca^{2+} channels in planar bilayers differ little in behavior from Ca^{2+} channels in cell-attached patches under matched experimental conditions. These direct comparisons have not been possible with Ca^{2+} channels from other systems that are inaccessible to patch-clamp analysis (*8, 9*). Incorporation of these channels into bilayers has allowed us to study Ca^{2+} channel activity under conditions that have not been achieved in intact cells, for example, at strongly positive potentials or with high intracellular divalent ions.

This method can also be used to answer questions about the influence of membrane and cytoplasmic components on Ca^{2+} channel activity. Activity of cardiac L-type Ca^{2+} channels disappears rapidly and irreversibly after the excision of a cell-attached patch (*2, 5, 15*). It is remarkable that after tissue homogenization in ordinary buffers and fractionation of membrane fragments, procedures requiring ~12 hours, calcium channels in bilayers are still active. However, as with an excised patch, there is a reduction in activity with time, seen either as a gradual decrease of the open probability or a sudden irreversible channel closure. It has been proposed that cyclic AMP–dependent protein phosphorylation is required to maintain active Ca^{2+} channels (*23*). Our results suggest that either a population of channels can remain in the phosphorylated state for several hours after tissue disruption, or that phosphorylation is not absolutely required for channel function. Furthermore, our results show that Ca^{2+} channels can undergo inactivation in the absence of intracellular components, indicating that inactivation is intrinsic to the channel molecule itself and does not require intracellular processes such as protein dephosphorylation (*24*). The precise role of cyclic AMP– or Ca^{2+}-dependent phosphorylation is one of the important issues that may be addressed with channels incorporated into bilayers (*25*).

REFERENCES AND NOTES

1. H. Reuter, *Nature (London)* **301**, 569 (1983); R. W. Tsien, *Annu. Rev. Physiol.* **45**, 341 (1983).
2. E. M. Fenwick, A. Marty, E. Neher, *J. Physiol. (London)* **331**, 599 (1982); S. Hagiwara and H. Ohmori, *ibid.* **336**, 649 (1983).
3. H. Reuter *et al.*, *Nature (London)* **297**, 501 (1982).
4. A. M. Brown *et al.*, *ibid.* **299**, 156 (1982).
5. A. Cavalie *et al.*, *Pfluegers Arch. Gesamte Physiol. Menschen Tiere* **389**, 284 (1983).
6. P. Hess *et al.*, *Nature (London)* **311**, 538 (1984).
7. H. Glossmann and D. Ferry, *Naunyn-Schmiedeberg's Arch. Pharmacol.* **323**, 279 (1983); B. Curtis and W. A. Catterall, *Biochemistry* **23**, 2113 (1984); M. Borsotto *et al.*, *Biochem. Biophys. Res. Commun.* **122**, 1357 (1984).
8. M. T. Nelson *et al.*, *Nature (London)* **308**, 77 (1984); B. E. Ehrlich *et al.*, *Science* **225**, 427 (1984).
9. H. Affolter and R. Coronado, *Biophys. J.* **48**, 341 (1985).
10. B. E. Ehrlich *et al.*, *J. Gen. Physiol.* **86**, 21a (1985); *Proc. Natl. Acad. Sci. U.S.A.* **83**, 193 (1986).
11. Bovine cardiac sarcolemmal vesicles [R. S. Slaughter, J. L. Sutko, J. P. Reeves, *J. Biol. Chem.* **258**, 3183 (1983); L. R. Jones, S. W. Maddock, H. R. Besch, *ibid.* **255**, 9771 (1983)] and rabbit skeletal muscle T-tubules [M. Rosemblatt *et al.*, *ibid.* **256**, 8140 (1981)] were prepared as described and stored frozen at −70°C for up to 4 months. Planar lipid bilayers were formed across a 200-μm-diameter hole in a polystyrene partition from decane solutions [P. Mueller and D. O. Rudin, *Curr. Top. Bioenerg.* **3**, 157 (1969)] of bovine brain phosphatidylethanolamine (10 mg/ml) and bovine brain phosphatidylserine (10 mg/ml) (Avanti Polar Lipids, Birmingham, AL). Membranes had resistances of 30 to 100 gigaohm and capacitances of 80 to 120 pF. Aqueous solutions were as described in the figure legends. Bay K 8644 was added to both chambers to a final concentration of 1 μ*M* from a 5 m*M* stock solution in ethanol. Vesicles were added to the cis chamber to a final concentration of 10 to 30 μg of protein per milliliter. Voltage clamp was applied with a patch-clamp amplifier modified for greater capacity compensation; currents were filtered at 200 Hz (−3 dB, 8-pole Bessel low pass), digitized at 1000 Hz, and stored in an PDP 11/23 computer.
12. For experiments with cardiac sarcolemma, the trans chamber was held negative with respect to the cis chamber and a depolarization resulted in the characteristic channel openings. Thus, the cis chamber (the side to which vesicles were added) represents the extracellular solution, consistent with conventional incorporation of right-side-out vesicles [L. R. Jones, S. W. Maddock, H. R. Besch, *J. Biol. Chem.* **255**, 9771 (1980)]. When skeletal muscle T-tubules were incorporated, channels were closed when the cis side was held negative with respect to the trans side, and depolarization increased channel activity. In this case, the cis chamber represents the cytoplasmic side. This is consistent with the incorporation of inside-out vesicles [H. Y. Lau *et al.*, *J. Gen. Physiol.* **74**, 335 (1979)].
13. M. Schramm *et al.*, *Nature (London)* **303**, 535 (1983).
14. S. Kokubun and H. Reuter, *Proc. Natl. Acad. Sci. U.S.A.* **81**, 4824 (1984); R. Ochi, N. Hino, Y. Niima, *Proc. Jpn. Acad. Ser. B Phys. Biol. Sci.* **60**, 153 (1984).
15. B. Nilius *et al.*, *Nature (London)* **316**, 443 (1985).
16. D. Mentrard, G. Vassort, R. Fischmeister, *J. Gen. Physiol.* **83**, 105 (1984); R. S. Kass and M. C. Sanguinetti, *ibid.* **84**, 705 (1984); K. S. Lee, E. Marban, R. W. Tsien, *J. Physiol. (London)* **364**, 395 (1985).
17. A. M. Brown, D. L. Kunze, A. Yatani, *Nature (London)* **311**, 570 (1984).
18. At the filtering frequency of 200 Hz, opening events of less than 1 msec were greatly attenuated. Thus, brief openings of L-type channels, and the activity of T-type channels (*15*) were probably lost.
19. M. T. Nelson, *Biophys. J.* **47**, 67a (1985).
20. P. Hess, J. B. Lansman, R. W. Tsien, *J. Physiol. (London)* **358**, 61P (1985); J. B. Lansman, P. Hess, R. W. Tsien, in preparation.
21. Permeability ratios were calculated according to $E_{reversal} = (RT/2F)\ln\{(4P_{Ba}a^o_{Ba})/(P_K a^i_K)\}$ where P_{Ba} is barium permeability, P_K is potassium permeability, a^o_{Ba} is the extracellular activity of barium, and a^i_K is the intracellular activity of potassium. [P. Fatt and B. L. Ginsborg, *J. Physiol. (London)* **142**, 516 (1958); K. S. Lee and R. W. Tsien, *ibid.* **354**, 253 (1984).]
22. P. Hess and R. W. Tsien, *Nature (London)* **309**, 453 (1984); W. Almers and E. W. McCleskey, *J. Physiol. (London)* **353**, 585 (1984); Y. Fukushima and S. Hagiwara, *ibid.* **358**, 255 (1985).
23. H. Reuter and H. Scholz, *J. Physiol. (London)* **264**, 49 (1977); N. Sperelakis and J. Schneider, *Am. J. Cardiol.* **37**, 1079 (1976).
24. R. Eckert and J. E. Chad, *Prog. Biophys. Mol. Biol.* **44**, 215 (1984).
25. D. A. Ewald, A. Williams, I. B. Levitan, *Nature (London)* **315**, 503 (1985).

26. We thank C. Miller, A. Fox, and E. McCleskey for many helpful discussions, A. Scriabine for providing Bay K 8644, and D. Ahrens for technical assistance. This work was supported by a research fellowship from the American Heart Association (Connecticut Affiliate) to R.L.R., and by grants from the Public Health Service, the Miles Institute, and Marion Laboratories.

28 October 1985; accepted 27 December 1985